Article

Measurement of the Dependence of Interfacial Charge-Transfer Rate Constants on the Reorganization Energy of Redox Species at n-ZnO/HO Interfaces

Thomas W. Hamann, Florian Gstrein, Bruce S. Brunschwig, and Nathan S. Lewis

J. Am. Chem. Soc., **2005**, 127 (40), 13949-13954• DOI: 10.1021/ja0515452 • Publication Date (Web): 16 September 2005

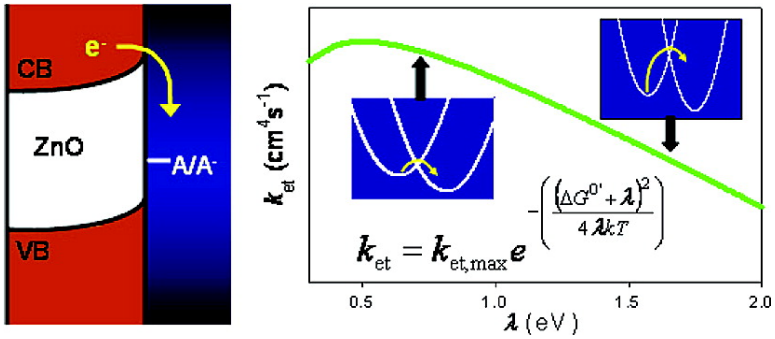

More About This Article

Additional resources and features associated with this article are available within the HTML version:

- Supporting Information
- Links to the 2 articles that cite this article, as of the time of this article download
- Access to high resolution figures
- Links to articles and content related to this article
- Copyright permission to reproduce figures and/or text from this article

View the Full Text HTML

J|A|C|S
ARTICLES
Published on Web 09/16/2005

Measurement of the Dependence of Interfacial Charge-Transfer Rate Constants on the Reorganization Energy of Redox Species at n-ZnO/H_2O Interfaces

Thomas W. Hamann, Florian Gstrein, Bruce S. Brunschwig, and Nathan S. Lewis*

Contribution from the Division of Chemistry and Chemical Engineering, 210 Noyes Laboratory, 127-72, California Institute of Technology, Pasadena, California 91125

Received March 10, 2005; E-mail: nslewis@caltech.edu

Abstract: The interfacial energetic and kinetics behavior of n-ZnO/H_2O contacts have been determined for a series of compounds, cobalt trisbipyridine ($Co(bpy)_3^{3+/2+}$), ruthenium pentaamine pyridine ($Ru(NH_3)_5py^{3+/2+}$), cobalt bis-1,4,7-trithiacyclononane ($Co(TTCN)_2^{3+/2+}$), and osmium bis-dimethyl bipyridine bis-imidazole ($Os(Me_2bpy)_2(Im)_2^{3+/2+}$), which have similar formal reduction potentials yet which have reorganization energies that span approximately 1 eV. Differential capacitance vs potential and current density vs potential measurements were used to measure the interfacial electron-transfer rate constants for this series of one-electron outer-sphere redox couples. Each interface displayed a first-order dependence on the concentration of redox acceptor species and a first-order dependence on the concentration of electrons in the conduction band at the semiconductor surface, in accord with expectations for the ideal model of a semiconductor/liquid contact. Rate constants varied from 1×10^{-19} to 6×10^{-17} cm^4 s^{-1}. The interfacial electron-transfer rate constant decreased as the reorganization energy, λ, of the acceptor species increased, and a plot of the logarithm of the electron-transfer rate constant vs $(\lambda + \Delta G^{\circ\prime})^2/4\lambda k_B T$ (where $\Delta G^{\circ\prime}$ is the driving force for interfacial charge transfer) was linear with a slope of ~ -1. The rate constant at optimal exoergicity was found to be $\sim 5 \times 10^{-17}$ cm^4 s^{-1} for this system. These results show that interfacial electron-transfer rate constants at semiconductor electrodes are in good agreement with the predictions of a Marcus-type model of interfacial electron-transfer reactions.

I. Introduction

Electron transfer across the semiconductor/liquid interface is one of the most fundamental processes in the operation of a photoelectrochemical energy conversion system. Control of the interfacial electron-transfer rate is required to optimize the solar energy conversion efficiency of such devices. Some of the factors that govern these interfacial electron-transfer rate constants, however, remain relatively poorly understood. While in principle semiconductor electrodes have advantages over metal electrodes in addressing some of the basic predictions of interfacial electron-transfer theories, such measurements are difficult because extraordinarily low defect densities at the semiconductor/liquid interface are required to prevent adsorption and surface-state related reactions from dominating the observed interfacial kinetics processes.[1,2]

Carefully prepared n-type ZnO/H_2O contacts with a series of $Os^{3+/2+}$ redox couples have recently been reported to exhibit the predicted dependence of interfacial charge-transfer rate constants, k_{et}, on changes in standard interfacial free energies, $\Delta G^{\circ\prime}$, for driving forces up to and beyond that of optimum exoergicity.[3] The rate constants were observed to decrease for high driving force contacts, indicating, by a straightforward application of Marcus theory,[4] that interfacial charge-transfer processes at some electrodes can operate in the inverted region.

This work addresses another basic prediction of the Marcus model for interfacial electron-transfer reactions at semiconductor electrodes. The interfacial electron-transfer rate constant should be strongly dependent on the reorganization energy, λ, of the acceptor species in solution. At constant driving force, in the normal region, k_{et} should decrease as λ increases. Previous measurements in our laboratory of the stability of n-Si/CH_3OH contacts as a function of the reorganization energy of the electron donor in the electrolyte provided indirect evidence of this prediction.[5] To directly verify this basic theoretical prediction, we have synthesized a series of one-electron redox couples having relatively constant potentials in the band-gap region of ZnO and having reorganization energies that span approximately 1 eV. Charge-transfer rate constants have been measured for these systems in contact with n-type ZnO electrodes. This investigation has provided a detailed comparison of interfacial electron-transfer reactions at an "ideally" behaving semiconductor/electrode interface with the predictions of Marcus theory for such systems.

(1) Lewis, N. S. *J. Phys. Chem. B* **1998**, *102*, 4843−4850.
(2) Lewis, N. S. *Annu. Rev. Phys. Chem.* **1991**, *42*, 543−580.
(3) Hamann, T.; Gstrein, F.; Brunschwig, B. S.; Lewis, N. S. *J. Am. Chem. Soc.* **2005**.
(4) Marcus, R. A. *Annu. Rev. Phys. Chem.* **1964**, *15*, 155−196.
(5) Pomykal, K. E.; Fajardo, A. M.; Lewis, N. S. *J. Phys. Chem.* **1995**, *99*, 8302−8310.

10.1021/ja0515452 CCC: $30.25

II. Experimental Section

A. Electrodes. The preparation of the ZnO electrodes has been described previously.[3] Electrochemical experiments reported in this work were confined to the Zn-rich surface. An area of 0.46 cm^2 was determined for the electrode used for data collection, with an estimated error of 0.03 cm^2.

Due to the limited number of high-quality ZnO single crystals available, a statistical approach was not feasible. At least two additional electrodes displayed similar energetic and kinetics features in measurements of all of the compounds reported here and produced nominally identical trends in the measured rate constants. All of the data reported herein were collected using a single electrode to minimize variation due to slight shifts in the flat-band potential of different electrode surfaces.

B. Electrolyte Solutions. Electrochemical experiments were carried out in an imidazole buffer prepared by adding 1 M HCl(aq) dropwise to 2.72 g of imidazole in 100 mL of H_2O until the desired pH was reached. The solution was then diluted to a volume of 500 mL (80 mM, pH = 6.5). The ionic strength, I, was adjusted to 1 M by addition of 37.4 g of KCl (Aldrich, 99+%) to provide the supporting electrolyte for electrochemical measurements.

C. Redox Compounds. Cobalt(II) chloride hexahydrate, cobalt(II) tetrafluoroborate hexahydrate, pentaamine chloro ruthenium(III) chloride, ammonium hexachloroosmate(IV), 1,4,7-trithiacyclononane (TTCN), pyridine (py), 2,2′-bipyridine (bpy), 4,4′-dimethyl 2,2′-bipyridine (Me_2-bpy), imidazole (Im), ammonium hexafluorophosphate, and tetrabutylammonium chloride (TBACl) were purchased from Aldrich and used as received. All solvents were reagent grade and were used as received. All compounds were prepared by modified literature procedures. The synthesis of $[Os(Me_2bpy)_2(Im)_2]Cl_2$ has been described previously.[3]

$[Co(bpy)_3](PF_6)_2$ was prepared by adding 1.7 g of $CoCl_2 \cdot 6H_2O$ in 50 mL of methanol to 6.4 g (3 equiv) of bpy dissolved in 100 mL of methanol.[5] The solution was stirred for 1 h. A stoichiometric amount of ammonium hexafluorophosphate was used to precipitate a yellow compound that was filtered and washed with ethanol, methanol, and ether. Elemental analysis yielded (calculated): C 43.91 (44.08), H 3.06 (2.96), N 10.23 (10.28). The chloride salt was made by dissolving $[Co(bpy)_3](PF_6)_2$ in acetone followed by addition of a stoichiometric amount of TBACl dissolved in acetone. The chloride salt that precipitated out of solution was filtered, washed with acetone and ether, and then dried under vacuum. Elemental analysis for $[Co(bpy)_3]Cl_2 \cdot 4H_2O$ yielded (calculated): C, 53.68 (53.74); H, 4.03 (5.11); N, 12.11 (12.53). Since chloride salts can adsorb water, water was added to the molecular formula to obtain agreement with the elemental analysis data. The compound composition was confirmed by NMR data on $Co(bpy)_3Cl_3$ that was prepared by oxidizing the parent compound with Cl_2(g) in D_2O.

$[Ru(NH_3)_5py](PF_6)_2$ was prepared by adding 9 mL of pyridine to 0.7 g of $[Ru^{III}(NH_3)_5Cl]Cl_2$ dissolved in 50 mL of 18 MΩ cm resistivity H_2O (Barnstead NANOpure) that had been purged with Ar(g) over approximately 10 g of Zn-amalgam.[6] The Ru(II) compound was precipitated by adding excess aqueous ammonium hexafluorophosphate and was collected by filtration, washed with ice-cold water and then with diethyl ether, and dried under vacuum. Elemental analysis yielded (calculated): C, 11.27 (10.81); H, 3.36 (3.63); N, 14.64 (15.13). The chloride salt was made by dissolving $[Ru(NH_3)_5py](PF_6)_2$ in acetone followed by addition of a stoichiometric amount of TBACl dissolved in acetone. The chloride salt immediately precipitated out of solution, was filtered, washed with acetone and ether, and was then dried under vacuum. The compound was further investigated using UV−vis spectroscopy and exhibited an absorption maximum at 407 nm.[6]

$[Co(TTCN)_2](BF_4)_2$ was prepared by adding 2 equiv, 0.36 g, of TTCN dissolved in 50 mL of ethanol to 0.34 g of $CoBF_4 \cdot 6H_2O$ dissolved in 50 mL of ethanol.[7] A purple precipitate was filtered, washed with ethanol and ether, and then dried under vacuum. Elemental analysis yielded (calculated): C, 24.12 (24.29); H, 3.62 (4.08). The compound composition was also confirmed by NMR data on $Co(TTCN)_2Cl_3$ that was prepared by oxidizing the parent compound with Cl_2(g) in D_2O.

The formal reduction potential of each compound, $E^{o\prime}$ (Table 2), was determined using cyclic voltammetry in buffered H_2O with 1 M KCl as the electrolyte. A glassy carbon disk electrode was used as the working electrode, a platinum mesh was employed as the counter electrode, and a standard calomel electrode (SCE) in a separate compartment was used as the reference electrode. Scans were taken from −0.4 V to 0.8 V vs SCE at a scan rate of 75 mV s^{-1}.

D. Electrochemical Measurements. Details of the electrochemical experiments have been described previously.[3] All experiments were carried out at room temperature. All potentials, E, are referenced to SCE. The oxidized, acceptor form, A, of each compound was created in situ via bulk electrolysis using a carbon mesh working electrode ([A] = 10 mM for $Co(bpy)_3^{3+}$, $Ru(NH_3)_5py^{3+}$, and $Co(TTCN)_2^{3+}$ and [A] = 5 mM for $Os(Me_2bpy)_2(Im)_2^{3+}$); a 5% error in [A] was estimated. The concentration of acceptor was varied by diluting a 1 mL aliquot of the redox solution with 9 mL of buffer. The Nernstian potential of the solution changed by less than 3 mV during each measurement and by less than 7 mV following dilution.

To deduce the space-charge capacitance at the ZnO electrode, impedance spectra were fitted to an equivalent circuit that consisted of the cell resistance, R_s, in series with two parallel components: the resistance to charge transfer, R_{sc}, and the space-charge capacitance, C_{sc}. Because C_{sc} is much less than the differential capacitance, C_{diff}, of either the Helmholtz layer or the double layer, C_{diff} was set equal to C_{sc}.[8] A linear regression was used to fit the A_s^2/C_{sc}^2 vs E data in accordance with the Mott−Schottky equation:[9]

$$\frac{A_s^{\,2}}{C_{sc}^{\,2}} = \frac{2}{q\epsilon_{ZnO}\epsilon_o N_d}\left(E - E_{fb} - \frac{k_B T}{q}\right) \tag{1}$$

where A_s is the surface area of the semiconductor electrode, k_B is Boltzmann's constant, T is the temperature, q is the charge of an electron (1.6022×10^{-19} C), ϵ_{ZnO} is the static dielectric constant of ZnO (8.65),[10] ϵ_o is the permittivity of free space, N_d is the dopant density of the semiconductor, and E_{fb} is the flat-band potential of the semiconductor/liquid contact. Values for N_D and E_{fb} were obtained from the slope and from the x-intercept adjusted by k_BT/q, respectively.

With knowledge of N_d and E_{fb}, the energy of the conduction band edge, $\mathbf{E}_{cb}$, was determined using the expression:

$$\mathbf{E}_{cb} = qE_{fb} + k_B T \ln\left(\frac{N_d}{N_c}\right) \tag{2}$$

where N_c is the effective density of states in the conduction band of the semiconductor ($N_c = 3.5 \times 10^{18}$ cm^{-3} for ZnO).[11] With knowledge of $\mathbf{E}_{cb}$, the electron concentration in the conduction band at the surface of the semiconductor, n_s, can be calculated at a given potential through the Boltzmann-type relationship:[1]

$$n_s = N_c e^{(\mathbf{E}_{cb} - qE)/k_B T} \tag{3}$$

Thus, application of a potential to an ideally behaving semiconductor

(6) Lavallee, D. K.; Lavallee, C.; Sullivan, J. C.; Deutsch, E. *Inorg. Chem.* **1973**, *12*, 570−574.
(7) Setzer, W. N.; Ogle, C. A.; Wilson, G. S.; Glass, R. S. *Inorg. Chem.* **1983**, *22*, 266−271.
(8) Fajardo, A. M.; Lewis, N. S. *J. Phys. Chem. B* **1997**, *101*, 11136−11151.
(9) Morrison, S. R. *Electrochemistry at Semiconductor and Oxidized Metal Electrodes*; Plenum: New York, 1980.
(10) Bhargava, R. *Properties of Wide Band gap II−VI Semiconductors*; Inspec: London, 1997; Series No. 17.
(11) Sze, S. M. *The Physics of Semiconductor Devices*; 2nd ed.; Wiley: New York, 1981.

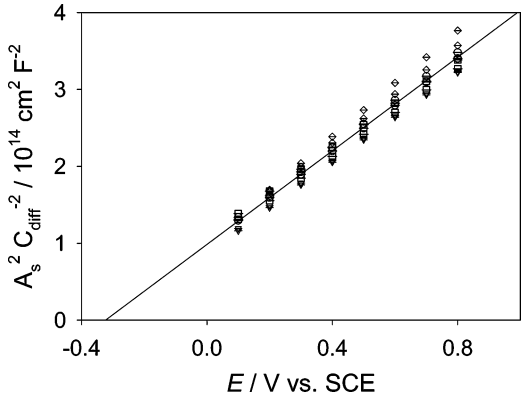

Figure 1. Mott−Schottky plots of ZnO in contact with $Co(bpy)_3^{3+/2+}$ (○), $Ru(NH_3)_5py^{3+/2+}$ (□), $Co(TTCN)_2^{3+/2+}$ (◇), and $Os(Me_2bpy)_2(Im)_2^{3+/2+}$ (▽) at high and low concentrations. The line indicates the least-squares fit of all of the data.

electrode interface effects a change in n_s, as opposed to changing the energetics of the interfacial charge-transfer process.

The J vs E data were obtained with a Schlumberger Instruments Electrochemical Interface Model SI1287 potentiostat. Two scans at a rate of 20 mV s^{-1} were measured for each system. At forward bias, the net flux of electrons from the conduction band to randomly dissolved acceptors in solution is given by[9]

$$J(E) = -qk_{et}[A]n_s \tag{4}$$

where k_{et} is the electron-transfer rate constant (cm^4 s^{-1}), and [A] is the acceptor concentration (cm^{-3}). The concentrations of the acceptor, [A], and n_s appear explicitly in the expression for the current density, thus yielding a second-order rate law for the charge-transfer process. Therefore, if J is shown to follow eq 4 and [A] is known, the value of k_{et} is readily calculated from the observed steady-state J vs E data.

III. Results and Discussion

A. Differential Capacitance vs Applied Potential Measurements. For each interface studied, Bode plots of the impedance magnitude, $|Z|$, vs the ac signal frequency, f, were linear over at least 2 orders of magnitude variation in frequency, with slopes ≈ -1 and phase angles of the current vs ac voltage $\approx -90°$. The observed impedance of these systems was thus dominated by a single capacitive circuit element, with $Z_{im} \approx (2\pi fC_{diff})^{-1}$.[8] The impedance spectra were fitted over the frequency range of 10^2 to 10^4 Hz to the equivalent circuit described above. The capacitance, C_{diff}, was independent of frequency, resulting in very small errors (<1%) for each fit. The series resistance of the system, R_s, was essentially constant for all measurements, with a value of 35 Ω.

Figure 1 displays Mott−Schottky plots in the form of A_s^2/C_{diff}^2 vs E for all contacts with varying concentrations of oxidized and reduced species grouped together. All of the Mott−Schottky plots were linear, as predicted by eq 1. Values for N_d and E_{fb} were obtained from the slope and intercept, respectively. The standard errors resulting from the fit were used to calculate the errors in N_d and E_{fb}, producing values of $E_{fb} = -0.35 \pm 0.01$ V vs SCE and $N_d = (5.5 \pm 0.6) \times 10^{16}$ cm^{-3}. Equation 2 was then used to calculate a value for $\mathbf{E}_{cb}/q = -0.46 \pm 0.01$ V vs SCE. The invariance of the capacitance data at a fixed electrode potential for all of the compounds is in accord with the "ideal" model of a semiconductor/liquid interface.

The nearly ideal behavior of the Mott−Schottky plots allowed accurate determination of the flat-band potentials for the ZnO/H_2O interfaces of interest. The E_{fb} values for a given ZnO/liquid contact did not vary significantly as the measurement frequency was changed. Our experimental value of $\mathbf{E}_{cb}/q = -0.46 \pm 0.01$ V vs SCE at pH = 6.5 is in very good agreement with prior results from our laboratory and from the work of others on ZnO in H_2O.[3,12,13]

B. Current Density vs Applied Potential Measurements. A notable feature of the ZnO/H_2O contacts reported herein is their excellent J vs E behavior. All of the junctions showed rectifying behavior, producing a limiting anodic current density and an exponentially increasing cathodic current density, in accord with the diode equation:

$$J = -J_0 e^{-[q(E-E(A/A^-))/\gamma k_B T]} \tag{5}$$

where J_o is the exchange current density and γ is the diode quality factor.

Figure 2 displays plots of $\ln(-J)$ vs E for all of the compounds investigated in this work. The diode quality factors were 1.2−1.3 at low concentrations of acceptors, indicating some relatively small but observable contribution from the presence of nonideal recombination pathways. Large acceptor concentrations, however, favor direct electron transfer. Diode quality factors were ≈1.1 at high acceptor concentrations, in accord with the expectation of $\gamma = 1$ for a process that is kinetically first-order in the concentration of electrons at the surface of the semiconductor. The dependence of the rate on the concentration of acceptor species in the solution was determined by decreasing [A] by a factor of 10. This decrease in acceptor concentration produced shifts of the J vs E data, ΔE, at a given current according to $\Delta E = (k_BT/q)\ln([A]_{low}/[A]_{high})$. The magnitude of the change in [A] was verified by measuring the limiting cathodic current densities at both acceptor concentrations, $J_{l,c,high}$ and $J_{l,c,low}$, with a Pt microelectrode. Values of γ and ΔE are given in Table 1 for the systems of interest in this work. In the series of measurements reported herein, the $J-E$ behavior for $Ru(NH_3)_5py^{3+/2+}$ shifted by less than the predicted −59 mV as the acceptor concentration was decreased; however, larger shifts were generally observed in other measurements with this couple, so the rate law was still taken to be a first-order process. The observed first order dependence of J on n_s and [A] validate the rate law of eq 4 and indicate that surface state effects do not dominate the charge-transfer processes of the systems investigated.[8]

C. Rate Constants for Interfacial Charge-Transfer, k_{et}. Because nondegenerately doped semiconductor electrodes show relatively little Frumkin effect associated with the liquid part of the solid/liquid double layer,[1] the acceptor concentration can be assumed to be equal to the bulk value. The surface electron concentration at each applied potential, $n_s(E)$, was computed according to eq 3 using the conduction band-edge energy extracted from the flat-band potential determinations (eq 2). The value of k_{et} was then calculated in accordance with the rate law given in eq 4, by dividing J by the quantity $\{-qn_s[A]\}$ at a given potential. The J vs E data collected at the largest acceptor concentration were used both to minimize the error in the concentration and because the diode quality factors were close to 1 under such conditions. The quoted k_{et} value for each contact represents the average of values calculated using potentials from

(12) Dewald, J. F. *J. Phys. Chem. Solids* **1960**, *14*, 155−161.
(13) Lohmann, F. *Ber. Bunsen-Ges. Phys. Chem.* **1966**, *70*, 428−434.

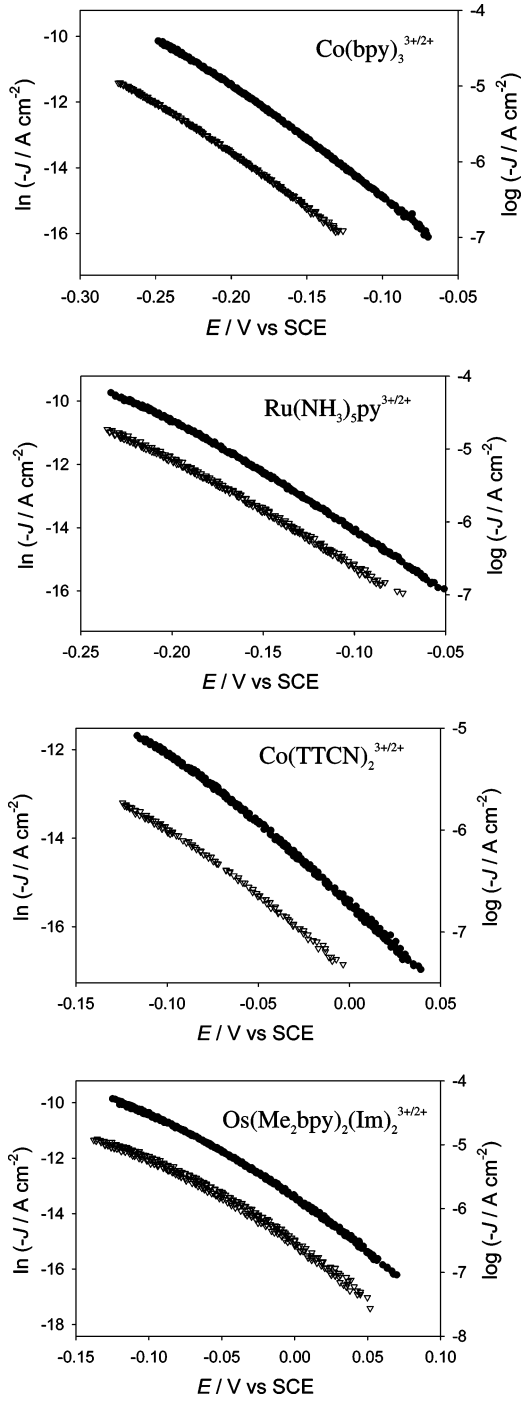

Figure 2. Plots of the dark current density, J, vs applied potential, E, for compounds at high concentration ([A] = 10 mM for $Co(bpy)_3^{3+/2+}$, $Ru(NH_3)_5py^{3+/2+}$, and $Co(TTCN)_2^{3+/2+}$ and [A] = 5 mM for $Os(Me_2bpy)_2(Im)_2^{3+/2+}$; ●) and low concentration ([A] ≈ 1 mM for $Co(bpy)_3^{3+/2+}$, $Ru(NH_3)_5py^{3+/2+}$, and $Co(TTCN)_2^{3+/2+}$, and [A] ≈ 0.5 mM for $Os(Me_2bpy)_2(Im)_2^{3+/2+}$; ▽). As noted in the text, a 10-fold decrease in [A] should result in a −59 mV shift of the $J-E$ curve. All potentials are referenced to SCE.

the high cathodic current density portion of the J vs E curve ($(-2$ to $-5) \times 10^{-6}$ A cm^{-2}) and, therefore, includes any effects of the deviation of the diode quality factor (typically 1.1 at the high redox species concentrations) from the ideal value of 1.0. A standard Gaussian error analysis was performed in conjunction with calculation of the rate constants by propagating the errors of all the measured parameters used in the calculation of k_{et}. The error in $\mathbf{E}_{cb}$ dominated the error in k_{et}, due to the exponential dependence of n_s on ($\mathbf{E}_{cb} - qE$). Table 1 summarizes the values of k_{et} determined for each of the ZnO/H_2O-redox couple junctions evaluated in this study.

D. Reorganization Energies. The total reorganization energy in self-exchange reactions is the result of changes in electronic configuration and in the bond lengths and angles in the inner-coordination sphere of the complexes, $\lambda_{se,in}$, and of changes in the polarization of the solvent in the outer-coordination sphere, $\lambda_{se,out}$. The total reorganization energy, λ_{se} (with $\lambda_{se} = \lambda_{se,in} + \lambda_{se,out}$), for a given species in a self-exchange electron-transfer process can be related to the self-exchange rate constant, k_{ex}, by the expression[14−18]

$$k_{ex} = K_A \kappa_{el} \nu_n \Gamma e^{-\lambda_{se}/4k_BT} \tag{6}$$

where K_A is the equilibrium constant for the formation of the precursor complex of the reactants, κ_{el} is the electronic transmission coefficient, ν_n is the effective nuclear vibration frequency of the activated complex, and Γ is a correction for nuclear tunneling. The precursor formation equilibrium constant for reactant pairs separated by the distance between r and $r + \delta r$ (cm) can be calculated as[16]

$$K_A(r) = \frac{4\pi N_A r^2 \delta r}{1000} e^{(-w(r)/k_BT)} \tag{7}$$

where N_A is Avogadro's number and $w(r)$ is the work required to bring the reactants to the separation distance, r. With the assumptions that the work is primarily Coulombic, the reactants are spherical, and the radii of the ions are equal ($r = 2a$, where a is the reactant radius), $w(r)$ is given by[16]

$$w(r) = \frac{z_1 z_2 q^2}{4\pi\epsilon_0\epsilon r(1 + \beta r I^{1/2})} \tag{8}$$

where z_1 and z_2 are the charges on the ions (2 and 3 for the redox couples of interest here), ϵ is the static dielectric constant of the medium (80.2 for H_2O at 20 °C[19]), and $\beta = (2N_A q^2/1000\epsilon_0\epsilon k_B T)^{1/2}$. The Debye−Hückel model is not expected to give quantitatively correct results as the ionic strength increases, particularly at the higher values of the ionic strength normally used in electrochemical experiments. However, $w(r)$ decreases as the ionic strength increases, so although the absolute value of the work calculated may be in error by a factor of 2 or more, the error in $K_A(r)$ is much smaller.

The frequency factor is given by[16]

$$\nu_n^2 = \frac{\nu_{out}^2 \lambda_{out} + \nu_{in}^2 \lambda_{in}}{\lambda_{out} + \lambda_{in}} \tag{9}$$

where ν_{out} and ν_{in} are the solvent and ligand stretching frequencies, respectively. For Os polypyridyl complexes, the inner sphere does not undergo significant changes upon electron

(14) Marcus, R. A.; Sutin, N. *Biochim. Biophys. Acta* **1985**, *811*, 265−322.
(15) Meyer, T. J.; Taube, H. In *Comprehensive Coordination Chemistry*; Wilkinson, S. G., Gilliard, R. D., McCleverty, J. A., Eds.; Pergamon Press: New York, 1987; Vol. 1, p 331.
(16) Sutin, N. *Acc. Chem. Res.* **1982**, *15*, 275−282.
(17) Sutin, N. *Prog. Inorg. Chem.* **1983**, *30*, 441−498.
(18) Brunschwig, B. S.; Logan, J.; Newton, M. D.; Sutin, N. *J. Am. Chem. Soc.* **1980**, *102*, 5798−5809.
(19) Lide, D. R., Ed. *CRC Handbook of Chemistry and Physics*, 81st ed.; CRC Press: 2001.

Table 1. Results from Current Density vs Applied Potential Measurements and Rate Constant Determinations[a]

compound	γ_{high}	γ_{low}	ΔE	$-\Delta G^{o\prime}$ (eV)	k_{et} ($cm^4\ s^{-1}$)	k_{et}^{calc} ($cm^4\ s^{-1}$)
$Co(bpy)_3^{3+/2+}$	1.1	1.2	−62	0.50 ± 0.01	$(1 \pm 0.6) \times 10^{-19}$	6.1×10^{-20}
$Ru(NH_3)_5py^{3+/2+}$	1.1	1.2	−38	0.49 ± 0.01	$(4 \pm 2) \times 10^{-19}$	2.5×10^{-18}
$Co(TTCN)_2^{3+/2+}$	1.1	1.3	−58	0.61 ± 0.01	$(5 \pm 3) \times 10^{-18}$	6.4×10^{-18}
$Os(Me_2bpy)_2(Im)_2^{3+/2+}$	1.1	1.3	−50	0.57 ± 0.01	$(6 \pm 4) \times 10^{-17}$	4.9×10^{-17}

[a] The quantities γ_{high} and γ_{low} are the diode quality factors at high and low acceptor concentration, respectively.

Table 2. Formal Potentials, $E^{o\prime}$, Self-Exchange Rate Constants, k_{ex}, and Reorganization Energies, λ, for the Redox Couples of Interest in This Work

	$E^{o\prime}$ (mV)[a]	k_{ex} ($M^{-1}\ s^{-1}$)	I (M)	a (Å)	K_A (M^{-1})	ν_n (s^{-1})	λ_{se} (eV)	$\lambda_{se,out}$ (eV)	$\lambda_{se,in}$ (eV)	$\lambda_{sc,out}$ (eV)	λ_{sc} (eV)
$Co(bpy)_3^{3+/2+}$	40	20[b]	0.1	6.5	0.28	10^{13}	2.64	0.60	2.04	0.49	1.51
$Ru(NH_3)_5py^{3+/2+}$	35	4.7×10^5[c]	1	4.2	0.12	10^{13}	1.52	0.93	0.59	0.76	1.06
$Co(TTCN)_2^{3+/2+}$	150	1.3×10^5[d]	0.2	5	0.14	10^{13}	1.67	0.75	0.92	0.62	1.08
$Os(Me_2bpy)_2(Im)_2^{3+/2+}$	110	8.7×10^7[e]	1	6.5	0.57	10^{11}	0.67	0.60	0.07	0.49	0.53

[a] Referenced to SCE. [b] Weaver, M. J.; Yee, E. L. *Inorg. Chem.* **1980**, *19*, 1936−1945. [c] Brown, G. M.; Krentzien, H. J.; Abe, M.; Taube, H. *Inorg. Chem.* **1979**, *18*, 3374−3379. [d] Chandrasekhar, S.; McAuley, A. *Inorg. Chem.* **1992**, *31*, 480−487. [e] Reference 3.

transfer,[20] and the reorganization energy is dominated by the solvent reorganization energy, so $\nu_n \approx \nu_{out} = 10^{11}\ s^{-1}$.[3,15,21] The other compounds of interest in this work have a significant inner-sphere contribution to the reorganization energy, hence $\nu_n \approx \nu_{in} = 10^{13}\ s^{-1}$.[16] All of the complexes studied are assumed to have similar values of $\kappa_{el} \approx 1$ (i.e., the reactions are adiabatic) and $\Gamma \approx 1$ (no significant tunneling contribution).[18] Values for k_{ex} are available from prior work, and the resulting values calculated for K_A, ν_n, and λ_{se} are given in Table 2.

The outer-sphere reorganization energy for two spherical reactants in solution can be calculated by[14]

$$\lambda_{se,out} = \frac{(\Delta zq)^2}{4\pi\epsilon_0}\left[\left(\frac{1}{a} - \frac{1}{R}\right)\left(\frac{1}{n^2} - \frac{1}{\epsilon}\right)\right] \qquad (10)$$

where Δz is the difference in the charge of the ions, R is the reactant center-to-center separation ($R = 2a$), and n is the refractive index of the solvent (1.3438 for 0.98 M KCl in H_2O at 20 °C[19]). The inner-sphere reorganization energy can be deduced by subtracting the outer-sphere reorganization energy from the total ($\lambda_{se,in} = \lambda_{se} - \lambda_{se,out}$). Values of a, $\lambda_{se,out}$, and $\lambda_{se,in}$ are given in Table 2.

The outer-sphere reorganization energy of a redox couple at a ZnO electrode, $\lambda_{sc,out}$, where both the redox couple in solution and the image charge in the semiconductor contribute to the total reorganization energy, is expected to be less than that for the self-exchange reaction of the couple in homogeneous solution. A theoretical value for the outer-sphere reorganization energy of a redox couple at a ZnO electrode can be calculated by[22−24]

$$\lambda_{se,out} = \frac{(\Delta zq)^2}{8\pi\epsilon_0}\left[\frac{1}{a}\left(\frac{1}{n^2} - \frac{1}{\epsilon}\right) - \frac{1}{2R_e}\left(\left(\frac{n_{ZnO}{}^2 - n^2}{n_{ZnO}{}^2 + n^2}\right)\frac{1}{n^2} - \left(\frac{\epsilon_{ZnO} - \epsilon}{\epsilon_{ZnO} + \epsilon}\right)\frac{1}{\epsilon}\right)\right] \qquad (11)$$

where n_{ZnO} is the refractive index of ZnO (1.9[10,25]) and R_e is the distance from the acceptor to the electrode ($R_e = a$).

The inner-sphere reorganization energy at a ZnO electrode is half of the value of $\lambda_{se,in}$, since half as many molecules participate in each electron-transfer event. The total reorganization energy for a redox couple at a ZnO electrode is therefore given by $\lambda_{sc} = (\lambda_{se} - \lambda_{se,out})/2 + \lambda_{sc,out}$. Values of $\lambda_{sc,out}$ and λ_{sc} for each of the redox couples are given in Table 2.

E. Dependence of Interfacial Charge-Transfer Rate Constants on Reorganization Energy: Comparison between Theory and Experiment. A nonadiabatic electronic coupling model, based on the Fermi Golden Rule applied to the case of a semiconductor electrode in contact with a random distribution of acceptor species in solution, has produced the following expression for the electron-transfer rate constant at a semiconductor/liquid interface:[26]

$$k_{et} = \frac{4\pi^2}{h}\frac{1}{(4\pi\lambda_{sc}k_BT)^{1/2}}\left\{\overline{H_{AB,sc}^2}\right\}\left\{\beta_{sc}{}^{-1}\right\}\left\{\frac{l_{sc}}{d_{sc}{}^{2/3}(6/\pi)^{1/3}}\right\}e^{\frac{-[(\overbrace{\mathbf{E}_{CB} - qE^{o\prime}}^{\Delta G^{0\prime}}) + \lambda_{sc}]^2}{(4\lambda_{sc}k_BT)}} \qquad (12)$$

where β_{sc} is the attenuation factor of the electronic coupling between the semiconductor and the redox species in the electrolyte, l_{sc} is the effective coupling length in the semiconductor, and d_{sc} is the atomic density of the solid. The quantity $\overline{H_{AB,sc}{}^2}$ represents the square of the matrix element that couples reactant and product states at energy **E**, averaged over all degenerate states in the semiconductor in a plane parallel to the electrode surface. This value is assumed to be independent of energy over the range of interest.[26] The interfacial free energy for charge transfer under standard conditions, $\Delta G^{o\prime}$, is computed by subtracting $qE^{o\prime}(A/A^-)$ from $\mathbf{E}_{cb}$. The subscript "sc" indicates parameters for a semiconductor electrode. Equation 12 can be rewritten as

(20) Biner, M.; Burgi, H. B.; Ludi, A.; Rohr, C. *J. Am. Chem. Soc.* **1992**, *114*, 5197−5203.
(21) Marcus, R. A. *J. Phys. Chem.* **1963**, *67*, 853−857.
(22) Marcus, R. A. *J. Phys. Chem.* **1990**, *94*, 1050−1055.
(23) Marcus, R. A. *J. Phys. Chem.* **1990**, *94*, 4152−4155.
(24) Kuciauskas, D.; Freund, M. S.; Gray, H. B.; Winkler, J. R.; Lewis, N. S. *J. Phys. Chem. B* **2001**, *105*, 392−403.
(25) Ashkenov, N.; Mbenkum, B. N.; Bundesmann, C.; Riede, V.; Lorenz, M.; Spemann, D.; Kaidashev, E. M.; Kasic, A.; Schubert, M.; Grundmann, M.; Wagner, G.; Neumann, H.; Darakchieva, V.; Arwin, H.; Monemar, B. *J. Appl. Phys.* **2003**, *93*, 126−133.
(26) Royea, W. J.; Fajardo, A. M.; Lewis, N. S. *J. Phys. Chem. B* **1997**, *101*, 11152−11159.

$$k_{et} = k_{et,max} e^{-(\Delta G^{\circ\prime}+\lambda_{sc})^2/4\lambda_{sc}k_B T} \quad (13)$$

where the prefactor has been combined into $k_{et,max}$, the rate constant at optimum exoergicity, obtained when $-\Delta G^{\circ\prime} = \lambda_{sc}$, with $k_{et,max} \approx 10^{-17}-10^{-16}$ cm^4 s^{-1}.[3,8,26] The value of $k_{et,max}$ is expected to be a weak function of the reorganization energy ($k_{et,max} \propto \lambda_{sc}^{-1/2}$) for nonadiabatic reactions and is independent of λ for adiabatic reactions. Any dependence of $k_{et,max}$ on $\lambda_{sc}^{-1/2}$ is therefore too small to be reliably observed in our experiments and is not included in this expression. Because all of the compounds are coupling to the same electrode, the electronic coupling coefficient, H_{AB}, for the interfacial electron-transfer reactions is likely to be similar for the various redox species of concern.

The expression for k_{et} in eq 13 can conveniently be written as

$$\ln k_{et} = \ln k_{et,max} - \frac{(-\Delta G^{\circ\prime} + \lambda_{sc})^2}{4\lambda_{sc}k_B T} \quad (14)$$

As shown in Figure 3, a plot of ln k_{et} vs $(\Delta G^{\circ\prime} + \lambda_{sc})^2/4\lambda_{sc}k_B T$ is linear, with a linear least-squares fit yielding a slope of -0.94 and an intercept of -38. The slope of -0.94 indicates adherence of the data to the Marcus model's prediction of the dependence of the interfacial electron-transfer rate constants on the reorganization energy and driving force of the reaction.[21−23] A value for $k_{et,max}$ can be derived from the intercept, yielding $k_{et,max} = 3 \times 10^{-17}$ cm^4 s^{-1}. This result is in reasonable agreement with the value of $k_{et} = 6 \times 10^{-17}$ cm^4 s^{-1} for $Os(Me_2bpy)_2(Im)_2^{3+/2+}$, which is essentially at maximal exoergicity, and with the theoretically predicted and experimentally determined value of $k_{et,max} = 10^{-17}-10^{-16}$ cm^4 s^{-1}.[3,8,26] Although both the $\Delta G^{\circ\prime}$ and λ_{sc} terms are included in eq 14 and Figure 3, for the redox couples investigated in this work $\Delta G^{\circ\prime}$ only varies by 0.1 eV while λ_{sc} varies by 1.0 eV. Prior work on ZnO electrodes has clearly elucidated the dependence of k_{et} on driving force at essentially constant reorganization energy of the redox species,[3] and the results described herein indicate satisfying agreement between theory and experiment for the dependence of k_{et} on the reorganization energy of the redox species involved in the interfacial charge-transfer process.

Another method to compare the data with Marcus theory is to calculate the interfacial rate constant expected at a given driving force and reorganization energy, assuming $k_{et,max} = 5 \times 10^{-17}$ cm^4 s^{-1}, according to eq 13. Values of the calculated rate constants, k_{et}^{calc}, corresponding to the $\Delta G^{\circ\prime}$ and λ_{sc} for each of the contacts in this study are given in Table 2. The calculated rate constant is within the error of values determined for k_{et} for the complexes $Co(bpy)_3^{3+/2+}$, $Os(Me_2bpy)_2(Im)_2^{3+/2+}$, and $Co(TTCN)_2^{3+/2+}$ and is approximately a factor of 6 larger than the measured k_{et} value for $Ru(NH_3)_5py^{3+/2+}$. In general, the agreement between theory and experiment within an order of magnitude is considered good, and in this context the agreement observed herein is excellent.

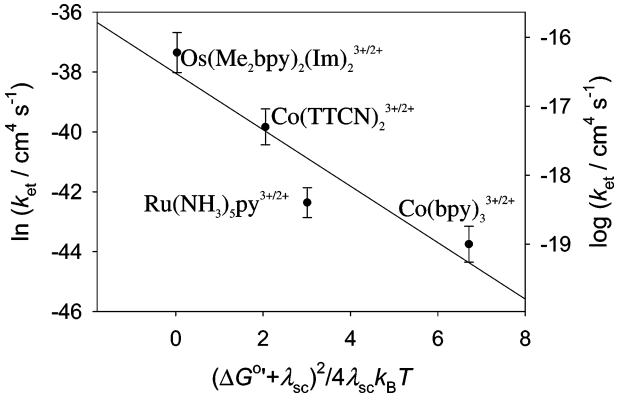

Figure 3. Plot of ln k_{et} as a function of the quantity $(\Delta G^{\circ\prime} + \lambda_{sc})^2/4\lambda_{sc}k_B T$ for the redox systems investigated. The solid line represents a linear least-squares fit of the data.

IV. Conclusions

The ZnO/H_2O junctions displayed nearly ideal energetic and kinetics behavior in contact with different redox couples. Current density vs potential measurements displayed a first-order dependence on the acceptor and surface electron concentrations. This behavior allowed for the straightforward experimental determination of the interfacial electron-transfer rate constants for such systems. The reorganization energy of the redox couples varied by approximately 1 eV and resulted in a change in k_{et} by a factor of 600. The data are thus in excellent agreement with the reorganization energy dependence of interfacial electron-transfer reactions predicted by the Marcus model of interfacial electron transfer at semiconductor electrode surfaces.

Acknowledgment. We acknowledge the Department of Energy, Office of Basic Energy Sciences, for support of this work.

JA0515452